Research on US-MRI fusion scheme based on non-negative matrix factorization and dual modality contrast agent

† M. Hou [1], * M. Y. Yang [1], X. T. Hu [1], N. N. Wang[1], W. H. Yu [2]
[1] School of Computer Science and Technology, Jiangsu Normal University, Xuzhou 221116, China.
[2] Jiangsu Key Laboratory of Education Big Data Science and Engineering, Xuzhou 221116,China.

†Corresponding author: 469954990@qq.com

Abstract

In order to realize the image fusion and improve the quality of the integration, by the aid of DMCA(dual modality contrast agent), a novel fusion method between US(ultrasound imaging) and MRI(magnetic resonance imaging) is put forward in the article. Due to US's strong speckle noise, it is an enormous challenge to fuse US with any other modality images. Under the circumstances, DMCA is used in both US and MRI to strengthen the most important information region of interest. Then, because of Rayleigh distribution of ultrasound imaging, an self-adaptive weighted non-negative matrix factorization(SWNMF) scheme is utilized to complete the fusion process. In view of the above-mentioned method, the multiple group comparison tests indicate that US-MRI fusion may be a remarkable method for gaining high-quality fusion image.

Keywords: US, MRI, fusion, DMCA, SWNMF

1. Introduction

US has been widely used in clinical diagnosis for its advantages of real-time and low-cost. Nowdays with the use of contrast agents, the quality of ultrasound imaging has been greatly improved [1,2]. However, the quality of US is mediocre compared its contrast with that of MRI or computed tomography (CT), because US is reflected very strongly when passing from gas to tissue, and vice versa.

MRI is another used commonly imaging modality with ideal soft-tissue contrast and high spatial resolution; besides particularly MRI can provide functional information needed by the clinic. Magnetic iron oxide nanoparticles owning superparamagnetic property can be used as a effective contrast agent for MRI to enhance its contrast [1]. One critical defect of MRI can't offer real-time motion-related images.

In a word, no single imaging modality holds all the merits satisfying all kinds of clinical needs, different imaging modalities have their respective advantages and disadvantages in clinical practice. In many circumstances, US and MRI are complimentary. Accordingly, it is ideal to fuse US with MRI. Owning to US's strong noise, it is a great challenge to fuse US with any other imaging modalities.

We have done prophase work on MRI-US registration and fusion based on DMCA, and have yielded some definite results [3~6]. The DMCA mentioned in the article is the dual-modality contrast agent, holding both US and MRI contrast function property. Microbubbles can be used as a effective contrast agent for US. Superparamagnetic iron oxide nanoparticles (SPIO) can be used as a powerful contrast agent for MRI. The combination of microbubbles and SPIO, DMCA, can be used as the contrast agent for both US and MRI because the DMCA can eliminate the defects of magnetic nanoparticles or microbubbles, respectively. Nowadays, effort to improve algorithms for medical image processing has seen very little progress [7~10].

The key contribution of this article is the introduction of the mentioned above DMCA to US-MRI fusion. Using DMCA prepared by Yang et al [1], this paper carries on the US-MRI fusion based on SWNMF, and arrivals at a conclusion that with the use of DMCA and SWNMF, fusion method performs well. The remainder of the paper is organized as follows: US-MRI fusion scheme (SWNMF) is described in Section 2. Section 3 provides several groups of comparison experiments, and analyzes the experimental results, while Section 4 concludes our paper.

2. Fusion method (SWNMF)

The noise distribution of ultrasonic imaging approximately conforms to Rayleigh distribution, because of which, SWNMF based on Rayleigh distribution is introduced as follows. Rayleigh distribution is defined as:

$$p_x(x) = \frac{2x}{a}\exp(-\frac{x^2}{a}) \ , \quad \text{s.t} \quad x \geq 0 \ . \tag{1}$$

For (1) a is a constant satisfied $a > 0$. To simplify the derivation process, a is set equal to 1 in the following section. If we now set $\frac{dp_x(x)}{dx} = 0$, we obtain $x = \frac{1}{\sqrt{2}}$. When x is set equal to $\frac{1}{\sqrt{2}}$, $p_x(x)$ reaches maximum value. According to Rayleigh distribution of the speckle noise of US, a new NMF is proposed as follows:

$$p(A_{ij} \mid U,V) = (A_{ij} - (UV)_{ij} + \frac{1}{\sqrt{2}})\exp(-(A_{ij} - (UV)_{ij} + \frac{1}{\sqrt{2}})^2) \tag{2}$$

For (2) A represents a given non-negative $n \times m$ matrix. This matrix is then approximately factorized into an $n \times r$ matrix U and an $r \times m$ matrix V.
Here we set

$$p(A \mid U,V) = \prod_{ij} p(A_{ij} \mid U,V) \tag{3}$$

then the maximum likelihood solution is the minimization of the loss function as follows

$$L(U,V) = \sum_{i,j} \left\{ \ (A_{ij} - (UV)_{ij} + \frac{1}{\sqrt{2}})^2 - \log(A_{ij} - (UV)_{ij} + \frac{1}{\sqrt{2}}) \ \right\} \tag{4}$$

To simplify (4), we add $\frac{1}{\sqrt{2}}$ to all elements of matrix A, and then (4) is written as

$$L(U,V) = \sum_{i,j} \left\{ \ (A_{ij} - (UV)_{ij})^2 - \log(A_{ij} - (UV)_{ij}) \ \right\} \tag{5}$$

We will derive below algorithm for the problem of WNMF which minimize the following weighted cost functions: the Weighted Rayleigh Distance

$$L_W(A \| UV) = \frac{1}{2}\sum_{i,j} W \circ \left\{ (A - UV)^2 - \log(A - UV) \right\} \tag{6}$$

where $W = \{W_{ij}\} > 0$ is a nonnegative weight matrix, and $X \circ Y$ is the Hadamard product (or element by element product) of the matrices X and Y. We only derive the updating rule for V since that of U can be infer in a similar fasion. We can consider the partial cost function for a single column of A, V and W, which we denote by a, v and w, respectively:

$$F(v) = F_w(a,Uv) = \frac{1}{2}\sum_i w_i \left\{ (a_i - [Uv]_i)^2 - \log(a_i - [Uv]_i) \ \right\} \tag{7}$$

$$=\frac{1}{2}\sum_i w_i(a_i-[Uv])^2+\frac{1}{2}\sum_i w_i\{-\log(a_i-[Uv]_i)\ \}$$

$$=\frac{1}{2}(a-Uv)^T D_W(a-Uv)+\frac{1}{2}w^T\{-\log(a-Uv)\}$$

$$=F_1(v)+F_2(v)$$

Where $$D_W=diag(w) \tag{8}$$

$$F_1(v)=\frac{1}{2}(a-Uv)^T D_w(a-Uv) \tag{9}$$

$$F_2(v)=\frac{1}{2}w^T\{-\log(a-Uv)\} \tag{10}$$

The first and two order derivatives of (9) and (10) can be obtained as (11)、(12) 、(13) and (14), respectively.

$$\nabla_v F_1(v^k)=-U^T D_w(a-Uv^k) \tag{11}$$

$$\nabla_v^2 F_1(v^k)=U^T D_w U \tag{12}$$

$$\nabla_v F_2(v^k)=\begin{pmatrix} w^T\dfrac{U_1}{a-Uv^k} \\ \vdots \\ w^T\dfrac{U_i}{a-Uv^k} \\ \vdots \\ w^T\dfrac{U_r}{a-Uv^k} \end{pmatrix}_{r\times 1} \tag{13}$$

$$\nabla_v^2 F_2(v^k)=\begin{pmatrix} w^T\left(\dfrac{U_1\circ U_1}{(a-Uv^k)\circ(a-Uv^k)}\right) & \cdots & w^T\left(\dfrac{U_1\circ U_i}{(a-Uv^k)\circ(a-Uv^k)}\right) & \cdots & w^T\left(\dfrac{U_1\circ U_r}{(a-Uv^k)\circ(a-Uv^k)}\right) \\ \vdots & \vdots & \vdots & \vdots & \vdots \\ w^T\left(\dfrac{U_i\circ U_1}{(a-Uv^k)\circ(a-Uv^k)}\right) & \cdots & w^T\left(\dfrac{U_i\circ U_k}{(a-Uv^k)\circ(a-Uv^k)}\right) & \cdots & w^T\left(\dfrac{U_i\circ U_r}{(a-Uv^k)\circ(a-Uv^k)}\right) \\ \vdots & \vdots & \vdots & \vdots & \vdots \\ w^T\left(\dfrac{U_r\circ U_1}{(a-Uv^k)\circ(a-Uv^k)}\right) & \cdots & w^T\left(\dfrac{U_r\circ U_k}{(a-Uv^k)\circ(a-Uv^k)}\right) & \cdots & w^T\left(\dfrac{U_r\circ U_r}{(a-Uv^k)\circ(a-Uv^k)}\right) \end{pmatrix}_{r\times r} \tag{14}$$

By iterating over (7) a number of partial differential iterations until the specified threshold is satisfied, we can obtain (15).

$$v^{k+1}=v^k-v^k\circ\frac{\nabla_v F_1(v^k)+\nabla_v F_2(v^k)}{(\nabla_v^2 F_1(v^k)+\nabla_v^2 F_2(v^k))v^k} \tag{15}$$

Where $\frac{X}{Y}$ is the Hadamard division (or element by element division) of the matrix X and Y.

Before fusion, the fused ultrasound and MRI are converted into column vectors $(k\times 1$, where $k=n\times m)$, respectively. Then the above two column vectors are then constructed into a $k\times 2$ matrix A, and the matrix is then approximately factorized into a $k\times 1$ column vector U and a 1×2 row vector V. Finally, when the iteration terminates, the $k\times 1$ vector U are then transformed into $n\times m$ matrix, namely gray level matrix of fusion image.

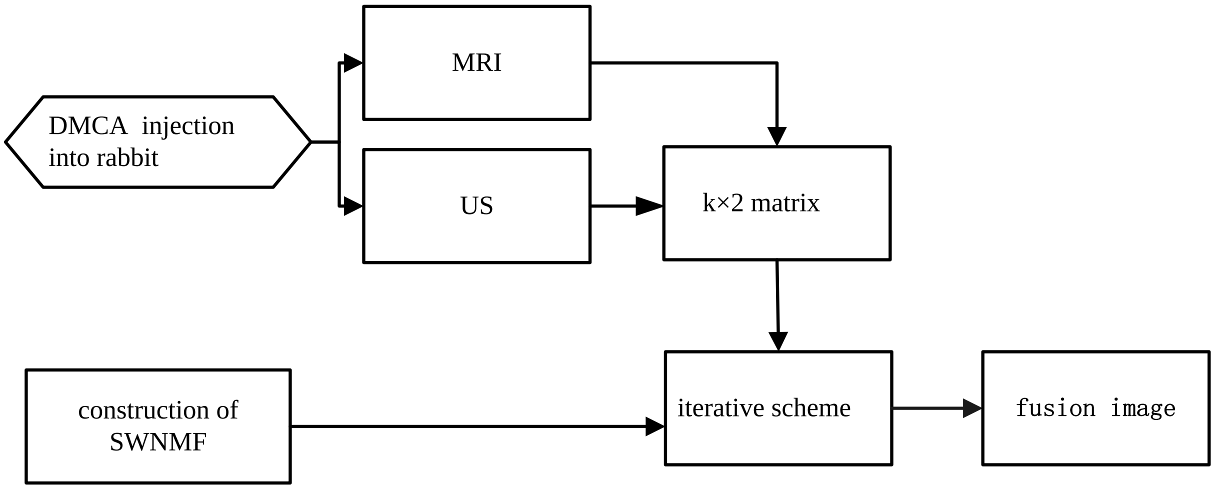

Figure 1. Flow chart of the proposed MRI-US fusion based on DMCA and SWNMF

In the process of image fusion, with the increasing of iterations, the fusion image pixel gray value is also real-time dynamic change result in that the gray distribution of each region of the image changes as well. So the weight corresponding to each region of the image should also change accordingly, and a fixed weight matrix does not reflect this dynamic process. In this paper, a iterative strategy is proposed, the weight matrix is dynamically adjusted according to the latest iterative results. The weighted coefficients of weight matrix reflect the importance of the corresponding pixels. When the iteration result has reached the target threshold, the adjustment of the corresponding weight coefficients is stopped. On the contrary, the weight coefficients are adjusted in the direction of the improvement of specific indicators.

3. Experiments

DMCA mentioned above is obtained from Jiangsu Key Laboratory for Biomaterials and Devices. DMCA can negatively strengthen T2-weighted (T2*WI) imaging signal. It can also enhance ultrasound backscattering echo intensity and positively increase the contrast and brightness of US.

Figure 2 include US and MRI fusion images without DMCA and with DMCA, respectively. As it can be intuitively observed from the perspective of fusion, Fig. 2 (c) has significant merits over Fig. 2 (c'). For better quantitative assessment, the four evaluation indexes AG (average gradient), EI (edge intensity), EN(Entropy) and SF(spatial frequency) are introduced. After fusion, performance evaluation with the use of DMCA had better improvement than that without DMCA. For example, AG, EI, EN and SF rises up from 2.0464 to 3.7630, from 22.5399 to 39.4881, from 6.5306 to 6.9099 and from 5.6550 to 10.2735 respectively. In short, the qualitative and quantitative analyses indicates that US-MRI fusion based on the above-mentioned method is effective.

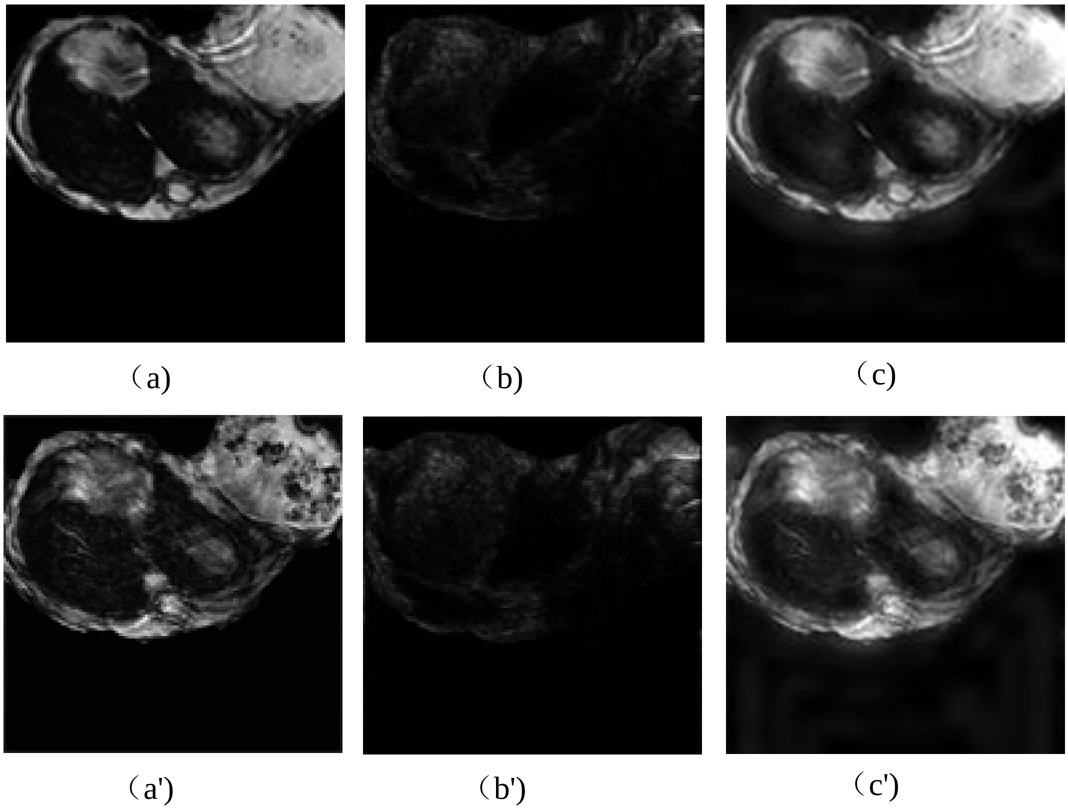

Figure 2. Fusion result comparison

(a)~(c) are MRI、US and fusion image without DMCA, respectively; (a')~(c') are MRI、US and fusion image with DMCA, respectively.

Table 1 Fusion result comparison

method category	evaluation indexes			
	AG	EI	EN	SF
the proposed method (without DMCA)	2.0464	22.5399	6.5306	5.6550
the proposed method (with DMCA)	3.7630	39.4881	6.9099	10.2735

4. Conclusions

As a new dual-modality contrast agent, DMCA is introduced into the field of medical image fusion. DMCA can enhance the texture details of medical imaging, which result in contrast improvement of important organization in the fusion image. Our fusion results are encouraging, However, they are still at preliminary stage. Further in vivo studies including toxicological and pathological studies will be necessary before our methods could be implemented in clinical applications.

References

[1] Yang, F. , Li, Y. X., Chen, Z. P., Zhang, Y., Wu, J. and Gu, N. (2009) Superparamagnetic iron oxide nanoparticle-embedded encapsulated microbubbles as dual contrast agents of magnetic resonance and ultrasound imaging, *Biomaterials* **30**, 3882–3890.

[2] Cai, X. W., Yang, F. and Gu, N. (2012) Applications of Magnetic Microbubbles for Theranostics, *Theranostics* **2**, 103–112.

[3] Hou, M., Luo, S. H., Yang, F., Ruan, X. B. and Gu, N. (2012) MRI-ultrasound registration based on dual modality contrast agent (in Chinese), *Chinese Science Bulletin* **57 (22)**, 2119-2126.

[4] Hou, M., Chen, C. X., Tang, D. L., Luo, S. H., Yang, F. and Gu, N. (2015) Magnetic microbubble-mediated ultrasound-MRI registration based on robust optical flow model, *BioMedical Engineering OnLine* **14(Suppl 1)**, S14.

[5] Hou, M., Luo, S. H., Yang, F., Ruan, X. B. and Gu, N. (2013) MRI- ultrasound fusion based on magnetic microbubble contrast agent (in Chinese), *Scientia Sinica (Informationis)* **43 (11)**, 1445-1459.

[6] Xiong, J., Luo, Y. and Tang, G. (2008) An Improved Optical Flow Method for Image Registration with Large-scale Movements, *Acta Automatica Sin* **34**, 760–764.

[7] Jung, E.M., Schreyer, A.G., Schacherer, D., Menzel, C., Farkas, S., Loss, M., Feuerbach, S., Zorger, N. and Fellner, C. (2009) New real-time image fusion technique for characterization of tumor vascularization and tumor perfusion of liver tumors with contrast-enhanced ultrasound, spiral CT or MRI: First results, *Clinical Hemorheology and Microcirculation* **43**, 57–69.

[8] Lindseth, F., Ommedal, S., Bang, J., Unsgård, G. and Nagelhus Hernes, T. A. (2001) Image fusion of ultrasound and MRI as an aid for assessing anatomical shifts and improving overview and interpretation in ultrasound-guided neurosurgery, *International Congress Series* **1230** 254–260.

[9] Schlaier, J. R., Warnat, J., Dorenbeck, U., Proescholdt, M., Schebesch, K. M. and Brawanski, A. (2004) Image fusion of MR images and real-time ultrasonography: evaluation of fusion accuracy combining two commercial instruments, a neuronavigation system and a ultrasound system, *Acta Neurochir (Wien)*, **146**, 271–277.

[10] Stone, M. (2005) A guide to analysing tongue motion from ultrasound images, *Clinical Linguistics and Phonetics* **19 (6-7)**, 455–502.